Optimum Estimation of Rain Microphysical Parameters From X-Band Dual-Polarization Radar Observables

John Kalogiros, Marios N. Anagnostou, Emmanouil N. Anagnostou, Mario Montopoli, Errico Picciotti, and Frank Silvio Marzano, *Senior Member, IEEE*

***Abstract*—Modern polarimetric weather radars typically provide reflectivity, differential reflectivity, and specific differential phase shift, which are used in algorithms to estimate the parameters of the rain drop size distribution (DSD), the mean drop shape, and rainfall rate. A new method is presented to minimize the parameterization error using the Rayleigh scattering limit relations multiplied with a rational polynomial function of reflectivity-weighted raindrop diameter to approximate the Mie character of scattering. A statistical relation between the shape parameter of the DSD with the median volume diameter of raindrops is derived by exploiting long-term disdrometer observations. On the basis of this relation, new optimal estimators of rain microphysical parameters and rainfall rate are developed for a wide range of rain DSDs and air temperatures using X-band scattering simulations of polarimetric radar observables. Parameterizations of radar specific path attenuation and backscattering phase shift are also developed, which do not depend on this relation. The methodology can, in principle, be applied to other weather radar frequencies. A numerical sensitivity analysis shows that calibration bias and measurement noise in radar measurements are critical factors for the total error in parameters estimation, despite the low parameterization error (less than 5%). However, for the usual errors of radar calibration and measurement noise (of the order of 1 dB, 0.2 dB, and 0.3 deg km^{-1} for reflectivity, differential reflectivity, and specific differential propagation phase shift, respectively), the new parameterizations provide a reliable estimation of rain parameters (typically less than 20% error).**

***Index Terms*—Dual-polarization weather radar, parameterization algorithms, rain microphysics, X-band.**

Manuscript received January 4, 2012; revised April 12, 2012 and June 25, 2012; accepted July 21, 2012. Date of publication September 17, 2012; date of current version April 18, 2013. This work is part of the HYDRORAD project (Research for SMEs category—Grand Agreement number FP7-SME-2008-1-232156) funded by EC 7th Framework Program from 2009 until 2011. Marios N. Anagnostou thanks the support of the Marie Curie Fellowship under the Grant Agreement Number 236871 HYDREX, coordinated by the Sapienza University of Rome, Italy, and the support of the Postdoctoral Fellowship by the Greek General Secretariat for Research and Technology under the Grant Agreement Number PE10(975) HYDRO-X, coordinated by the National Observatory of Athens, Greece, in the framework of the program "Education and Lifelong Learning" funded by Greece and EU-European Social Fund.

J. Kalogiros is with the Institute of Environmental Research and Sustainable Development, National Observatory of Athens, 11810 Athens, Greece (e-mail: jkalog@noa.gr).

M. N. Anagnostou is with the Institute of Environmental Research and Sustainable Development, National Observatory of Athens, Athens, Greece, and the Department of Information Engineering, Sapienza University of Rome, 00185 Rome, Italy (e-mail: ma111@engr.uconn.edu).

E. N. Anagnostou is with the Department of Civil and Environmental Engineering, University of Connecticut, Storrs, CT 06269 USA (e-mail: manos@engr.uconn.edu).

M. Montopoli is with the Department of Geography, University of Cambridge, Cambridge CB2 1TN, U.K., and the Centro di Eccellenza per l'integrazione di tecniche di Telerilevamento E Modellistica numerica per la Previsione di eventi meteorologici Severi (CETEMPS) Center of Excellence, University of L'Aquila, 67040 L'Aquila, Italy (e-mail: mario.montopoli@gmail.com).

E. Picciotti is with the CETEMPS Center of Excellence, University of L'Aquila, 67040 L'Aquila, Italy (e-mail: errico.picciotti@himet.it).

F. S. Marzano is with the Department of Information Engineering, Sapienza University of Rome, 00185 Rome, Italy, and the CETEMPS Center of Excellence, University of L'Aquila, 67040 L'Aquila, Italy (e-mail: marzano@diet.uniroma1.it).

Digital Object Identifier 10.1109/TGRS.2012.2211606

I. Introduction

A MAJOR objective of dual-polarization weather radars is the quantitative estimation of rainfall rate and drop size distribution (DSD) parameters. In addition to radar reflectivity (Z_h) at horizontal polarization, these dual-polarization radars provide, among other parameters, the differential reflectivity (Z_{dr}) and the specific differential propagation phase shift (K_{dp}), which is calculated from differential phase shift (Φ_{dp}) measurements. The two latter observables are the anisotropic result of the non-spherical shape of raindrops on backscatter (Z_{dr}) and forward propagation (K_{dp}) of electromagnetic waves with horizontal and vertical polarization components in rain [1]. According to measurements in rain, differential reflectivity Z_{dr} has been found to be related mainly to the raindrop size [2], [3], which is typically characterized by the median volume diameter D_0, whereas K_{dp} is closely related to rainwater content, mean drop shape, which is characterized by the drop axis ratio and the standard deviation of the orientation angle of drops (zero average value in rain) [1], [4].

A combination (algorithm) of the radar measurements Z_h, Z_{dr}, and K_{dp} is usually utilized to estimate the parameters of a theoretical (best-fitted) raindrop DSD, such as the normalized Gamma distribution [5], [6], as well as the mean drop shape, rainfall rate, and specific attenuation coefficient [7]–[14]. Due to the complexity of scattering by rain, there are no closed-form physical models that can be used for this estimation. Retrieval algorithms are usually developed by fitting the results from numerical simulations of scattering performed over the expected range of DSD parameters, drop shape models, distribution of the orientation of drop's symmetry axis (canting angle), and environmental conditions (air temperature) to predefined polynomial or power functions of radar measurements (with unknown parameters to be determined by the best fit). These parameterizations are actually affected by a considerable error

bias and standard deviation [1], [5], [8]–[11], [13]–[16] so that it would be desirable to improve them to minimize the total error, which also includes the measurement error.

This work presents a methodology to objectively define the optimal parameterization functions that minimize the approximation error using radar scattering simulations as a reference for a wide range of physical parameters and measurement errors. The focus on X-band applications is due to the increased interest in recent years for the use of X-band polarimetric radars in rainfall studies [10], [11], [13]–[16], due to their advantages like low cost, small size and mobility, high resolution, and increased sensitivity to light rain. However, the proposed methodology can be easily applied to radar observables at other radar frequencies (for example, C band and above frequencies) with similar results. The paper is organized as follows. After the introduction of rain parameters and radar observables in Section I, in Section III, the proposed methodology to define optimal parameterizations with minimum approximation error is described, and in Section IV, these methods are applied for the Mie-parameterized retrieval of rain parameter from X-band dual-polarization observations. This section also describes the effects due to model calibration and measurements errors and evaluates the method against radar parameters derived from disdrometer measurements. Conclusions are summarized in Section V.

II. Rain Microphysical Parameters and Radar Observables

The rain DSD, the shape of the raindrops, and their orientation and air temperature in the radar sampling volume are the parameters that control the scattering of electromagnetic waves by raindrops. The DSD for a time period of some minutes has been found to satisfactorily follow the Gamma distribution [17]

$$n(D) = N_0 D^{\mu} \exp(-\Lambda D) \tag{1}$$

where D is the equivalent (due to the non-spherical shape) volume diameter of raindrops with units mm and N_0, μ and Λ are parameters of the volume density $n(D)$ with units $\mathrm{m}^{-3}\mathrm{mm}^{-1}$. An equivalent to (1) is the normalized Gamma distribution proposed by [5], [6], and [18]

$$n(D) = N_w f(\mu) \left(\frac{D}{D_0}\right)^{\mu} \exp\left[-(\mu+3.67)\frac{D}{D_0}\right] \tag{2a}$$

where

$$f(\mu) = \frac{6}{3.67^4}\frac{(3.67+\mu)^{\mu+4}}{\Gamma(\mu+4)} \tag{2b}$$

and the intercept parameter (N_w) now has units which do not depend on the shape parameter μ in contrast to N_0. The median volume diameter (D_0) is defined by

$$\int_0^{D_0} D^3 n(D) dD = \frac{1}{2} E[D^3] \tag{3}$$

where E stands for the expectation value, which in practice is estimated as the DSD-weighted integral over the whole range of diameter values. Another frequently used measure of raindrop diameter is the mass-weighted mean diameter $D_m = E[D^4]/E[D^3]$, which is related to D_0 with the relation $D_m = D_0(\mu+4)/(\mu+3.67)$. Rain parameters can be expressed in terms of DSD: an example is the rainfall rate $R = (\pi/6)E[v(D)D^3]$, where $v(D)$ is the terminal velocity of raindrops expressed as a power or an exponential function of their sphere-equivalent diameter [1].

The equilibrium shape of raindrops is considered to be an oblate spheroidal with an axis ratio $r = b/a$ (b and a are the lengths of the minor and major axes, respectively) determined by the balance of hydrostatic, surface tension, and aerodynamic forces, but in reality raindrops exhibit steady-state oscillations [4]. The axis ratio is usually modeled as a linear or higher degree polynomial function of drop diameter. In this paper, the model of [19], which is supported by recent observations [20], is used

$$r = 1.0048 + 5.7\times10^{-4}D - 2.628\times10^{-2}D^2 + 3.682 \times10^{-3}D^3 - 1.677\times10^{-4}D^4 \tag{4}$$

where D is in mm, and it is usually in the range 0–7 mm. A linear model of axis ratio $r = (1+0.5\beta) - \beta D$ ($r = 1$ for $D < 0.5$ mm) is also commonly used as in [15], where the value of the slope parameter β is about 0.066 mm^{-1} (equilibrium value). This equilibrium value is obtained by fitting the linear model of axis ratio to (4). In addition, raindrops tend to fall with an orientation angle (the canting angle in the plane of polarization of the incident electromagnetic wave) of their minor symmetry axis with respect to the vertical direction due to atmospheric turbulence [21] or an effective canting angle due to drop oscillations [4]. Assuming a Gaussian model with zero mean the standard deviation of canting angle, the distribution of the latter is typically in the range 5°–10° [1]. More precisely and particularly for wide distributions with large standard deviations, the orientation angles follow a Fisher distribution because they correspond to the orientation of the symmetry axis which is represented by a 3-D vector [1].

Using the above parameterizations of DSD, axis ratio and canting angle distribution, it is possible to simulate radar observables (Z_h, Z_{dr}, and K_{dp}) in a radar volume using the T-matrix method for numerical simulations of the scattering of electromagnetic waves by spheroidal water raindrops [22], [23]. For Rayleigh scattering (limit of small drop diameter compared to wavelength), zero canting angle, and ignoring constants of proportionality, it can be shown that (see Chapter 7 of [1])

$$Z = 10^{0.1Z_h} \approx E\left[\frac{D^6}{r^{\frac{7}{6}}}\right] \approx \frac{E[D^6]}{r_z^{\frac{7}{6}}} \tag{5a}$$

$$\xi_{dr} = 10^{0.1Z_{dr}} \approx \frac{E[D^6]}{E\left[r^{\frac{7}{3}}D^6\right]} \approx \frac{1}{r_z^{\frac{7}{3}}} \tag{5b}$$

$$K_{dp} \approx E[D^3(1-r)] \approx E[D^3](1-r_m) \tag{5c}$$

where the symbol $\approx$ denotes approximation, Z (units mm^6 m^{-3}) and ξ_{dr} (simple ratio) are the linear horizontal and differential reflectivity, respectively (note that Z_h will be

expressed through the reflectivity Z in the rest of the paper) and r_z and r_m are the reflectivity-weighted and mass-weighted mean axis ratios, respectively

$$r_z = \frac{E(rD^6)}{E(D^6)} \tag{6a}$$

$$r_m = \frac{E(rD^3)}{E(D^3)}. \tag{6b}$$

In addition within the Rayleigh limit following the same approach as in [1] the specific horizontal attenuation in rain A_h, the specific differential attenuation A_{dp} and the backscattering differential phase shift δ_b (which contributes to the measured differential phase shift Φ_{dp}) can be shown to be

$$A_h \approx E\left[\frac{D^3}{r^{\frac{7}{6}}}\right] \approx \frac{E[D^3]}{r_m^{\frac{7}{6}}} \tag{7a}$$

$$A_{dp} \approx E\left[D^3\left(1/r^{\frac{7}{6}} - r^{\frac{7}{6}}\right)\right] \approx E[D^3]\left(1/r_m^{\frac{7}{6}} - r_m^{\frac{7}{6}}\right) \tag{7b}$$

$$\delta_b \approx E\left[\frac{(1-r)}{r^{\frac{3}{7}}}\right] \approx \frac{[1-E(r)]}{E(r)^{\frac{3}{7}}}. \tag{7c}$$

The functions $E(D^3)$, which is the water content W with the omission of the constant $(\pi/6)\rho_w$ where ρ_w is the water density, and $E(D^6)$ can be estimated from the DSD given in (2a) as

$$E(D^\nu) = F_\nu(\mu) N_w D_0^{\nu+1} \tag{8a}$$

for $\nu = 3$ and 6, where

$$F_\nu(\mu) = f(\mu)\Gamma(\mu+\nu+1)/(\mu+3.67)^{\mu+\nu+1} \tag{8b}$$

and Γ indicates the Gamma function. To simplify calculations, the mean axis ratios r_z, r_m, and $E(r)$ may be assumed to be approximately equal. This is justified because the purpose of this section is to qualitatively define the Rayleigh-limit relations of radar observables. The small effect of this approximation on the accuracy of the parameterizations, which are derived in the next sections, is verified by the small parameterization error obtained according to the numerical tests. Furthermore, to estimate an effective mean slope parameter (β_e), it may be assumed that the axis ratio follows the linear model. Rayleigh approximation is not valid at high frequencies like X-band, but it can provide a useful base to understand the dependence of radar measurements on DSD parameters and raindrops shape.

III. Methodology to Parameterize Mie Effects in Radar Rain-Retrieval Algorithms

The Rayleigh-limit relations, presented in the previous section, can be combined to estimate rain parameters from polarimetric radar measurements of Z_h, Z_{dr}, and K_{dp}. Using (5a)–(5c) and (8a) and (8b). It can be shown analytically that

$$D_0 = \left[\frac{F_3(\mu)}{F_6(\mu)}\frac{Z_h}{K_{dp}}\xi_{dr}^{-1/2}\left(1-\xi_{dr}^{-3/7}\right)\right]^{\frac{1}{3}}. \tag{9}$$

To check the application of this relation at X-band (9.37 GHz), T-matrix scattering simulations were carried out for all possible combinations (equally weighted) of rain parameters in wide value ranges

$$\begin{aligned} 1 \le \log_{10}(N_w) \le 5 (\mathrm{m}^{-3}\ \mathrm{mm}^{-1}) \\ 0.5 \le D_0 \le 3.5 (\mathrm{mm}) \\ -1 \le \mu \le 5 \end{aligned} \tag{10}$$

with an increment of 0.1 for $\log_{10}(N_w)$ and D_0 and 1 for μ. The drop diameter values used in the DSD calculations have a range from 0.1 to 10 mm (taking into account the theoretical corrections for truncation errors of the DSD moments) and a resolution of 0.1 mm. The following physical and practical constraints were used to exclude combinations of the simulation parameters that give unrealistic radar observables

$$\begin{aligned} Z_h &\le 65\ (\mathrm{dBZ}) \\ 0.2 \le K_{dp} &\le 20\ (\mathrm{deg\ km}^{-1}) \\ R &\le 300\ (\mathrm{mm\ h}^{-1}). \end{aligned} \tag{11}$$

The elevation of the radar antenna was assumed to be 1° (that is a typical operational value close to zero), air temperature T at 10 °C, a Fisher distribution with a standard deviation of 7.5° for canting angle distribution, and raindrops axis ratio given by (4). However, to include the effect of possible deviations of axis ratio from this model, an effective mean slope parameter (β_e) in the range 0.026 to 0.106 mm^{-1} with an increment of 0.01 mm^{-1} was used by redefining axis ratio as $r_e = 1-(1-r)\beta_e/0.066$, where 0.066 mm^{-1} is the equilibrium value of slope parameter, and an upper value of unity. In this way, the function of axis ratio against raindrop diameter moves above or below (4), depending on β_e while keeping its shape. The wide range of the simulation parameters N_w, D_0, μ, and β_e aim to the development of parameterizations that are characterized by small error even at extreme values of these parameters.

Fig. 1(a) shows that the right-hand part of (9) for various values of μ at X-band is not a linear function of D_0, as expected due to the Mie character of scattering at these electromagnetic frequencies. The functions $F_3(\mu)$ and $F_6(\mu)$ are not included in the analysis, but even if they were included, the lines for the various μ values do not collapse in one straight line as it would be the case for Rayleigh scattering. To parameterize the nonlinear effects of the Mie character of scattering at X-band, a direct approach is to add to the right hand of (9) and generally to the Rayleigh-limit relations a multiplicative factor which could be a rational polynomial function of raindrops diameter. Rational polynomial functions are able to approximate quite accurately complex functions. The median volume diameter D_0 could be used to represent the mean raindrops diameter, but the reflectivity-weighted mean diameter $D_z = E[D^7]/E[D^6]$ can be estimated with a single relation by radar observables irrespective of the unknown parameter μ as it is shown in Fig. 1(b). The reflectivity-weighted mean diameter D_z is related to D_0 with the relation $D_z = D_0(\mu+7)/(\mu+3.67)$ for a normalized Gamma DSD. The removal of the direct effect of μ is due in part to the fact that $[D_0 F_6(\mu)/F_3(\mu)]^{1/3}$ tends to D_z for large values of μ, and it should be expected because the reflectivity is the dominant radar measurement. This is desirable in parameterizations because there are more independent rain parameters to estimate (N_w, D_0, μ, and β_e) than the three

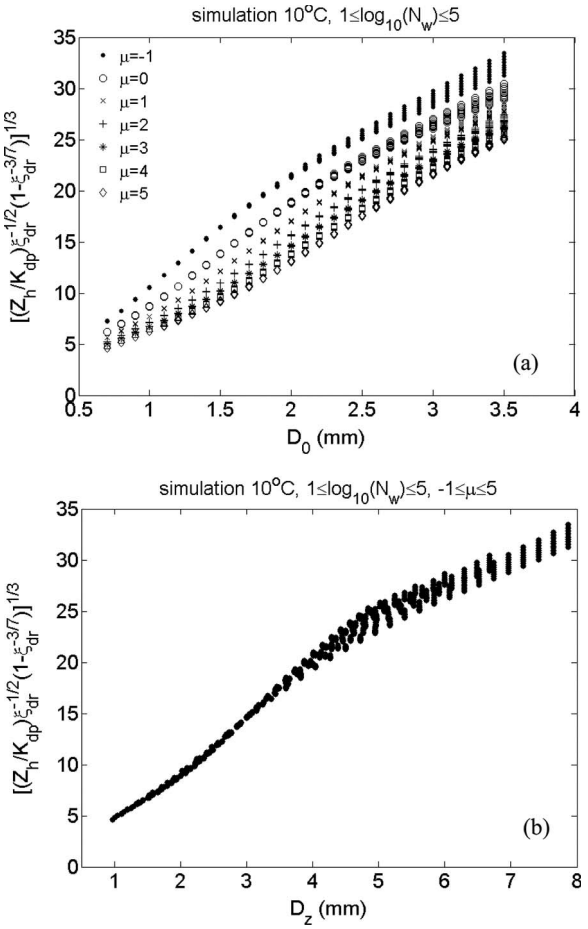

Fig. 1. Correlation of the right-hand part of (9) against (a) median volume diameter D_0 and (b) reflectivity-weighted mean diameter D_z of raindrops from scattering simulations at X-band. The units of K_{dp} and Z_h are deg km^{-1} and mm^6 mm^{-3}, respectively, while ξ_{dr} (ratio) has no units.

radar measurements Z_h, Z_{dr} and K_{dp} (input variables in the parameterizations).

In addition, the use of D_z, as representative of raindrops diameter, removes most of the dependence of the relations for estimation of the parameters A_h, A_{dp}, δ_b, and β_e on μ, as it is shown in Fig. 2. The functions of radar measurements, which are used to scale these parameters, can be found from (5)–(8) in a similar way as (9) with a change of exponents with value 0.5 to 0.2 in the scaling functions of A_h and A_{dp} to minimize the scatter of data. This indicates that the values of the exponents in these functions, as well as the constants of proportionality, should be estimated by a fitting procedure (the best fit criterion was the minimum mean squared error) to minimize the scatter of the approximations but keeping the form of dependence on $Z_{\rm h}$, K_{dp}, and ξ_{dr}. The fitting procedure should also give an estimation of the coefficients and the degree of the rational polynomial functions of D_z, which describe the Mie character of scattering as mentioned above.

For the rest of parameters to be estimated (the DSD parameters D_0, N_w, μ, and rainfall rate R), an additional constraint is needed. Disdrometer data from various geographical locations indicate that the DSD is a constrained Gamma distribution where the shape parameter μ of the DSD, which is connected to the width of the DSD, is related to D_0 or equivalent to the parameter Λ of the DSD [24], [25]. Fig. 3 shows data from a bidimensional-video disdrometer (2-D-VD) which was operating in Athens, Greece for about 6 years in the time period 2002–2009. The disdrometer recorded DSD data in time intervals of about 1 min within a diameter range 0.1 to 10 mm and with a resolution of 0.2 mm. To exclude noisy data only, the DSDs corresponding to rainfall rates $R > 3$ mm h^{-1} and number density of raindrops $N_d > 10$ m^{-3} were used. The DSD parameters N_w and D_m were computed using the DSD moments method [4] applied to the measured distributions in time periods of 1 min. The shape parameter was not estimated with a similar moments method because this involves estimation of high-order moments of the DSD (up to fifth or sixth-order moment), which are characterized by large error due to the measurement errors in the high tail (high raindrop diameter values) of the DSD. Thus, the shape parameter was estimated by the best fit of the normalized Gamma distribution (2a) to the measured DSD. The estimates of N_w and D_m with best fit of the normalized Gamma distribution to the measured DSD gave frequent outliers, while the moments method for the estimation of these parameters was more robust. These disdrometer data support the idea of a constrained Gamma DSD and agree with [25] for D_0 values less than 2 mm. The limit of μ at higher D_0 values is a little higher than that of [25]. However, their approach was to fit a second degree polynomial of μ to the Λ parameter which does not favor the accurate estimation of the limit of μ at large D_0 values. A fit of an exponential function of μ against D_0 with a lower limit of -1, which is indicated by the measured data, is

$$\mu = 165e^{-2.56D_0} - 1. \tag{12}$$

An exponential function is used to describe adequately the observed trend of μ to a steady value at large D_0 values. This correlation of μ with D_0 is the additional constraint which is needed for the estimation of D_0, N_w and μ from radar measurements. An additional measurement which is usually available from polarimetric radars (like the co-polar correlation coefficient ρ_{hv}) might be considered to remove this constraint. The co-polar correlation coefficient ρ_{hv} depends on the reflectivity-weighted variance and mean values of axis ratio [1], and after some simplifying assumptions, it can be shown that ρ_{hv} depends directly mainly on D_z and Z_{dr} and a lot less on μ (as T-matrix simulations at X-band also indicate). Thus, in practice, the usage of ρ_{hv} to remove the above $\mu - D_0$ constraint in rain parameterizations is not advisable because highly accurate (an accuracy of ρ_{hv} at about 0.001 [1]) and very low noise radar measurements of ρ_{hv} would be needed.

IV. Optimal Parameterizations for X-Band Polarimetric Estimation of Rain Parameters

T-matrix scattering simulations at X-band were carried out for a wide range of rain parameters and constraints, as described above in (10) and (11) with the addition of constrained μ (the exponential function $\mu(D_0)$ in Fig. 3 instead of varying μ in the range -1 to 5), D_z was limited in the range 0.5 to 8 mm, and air temperature at 10 °C. Using the methodology described in

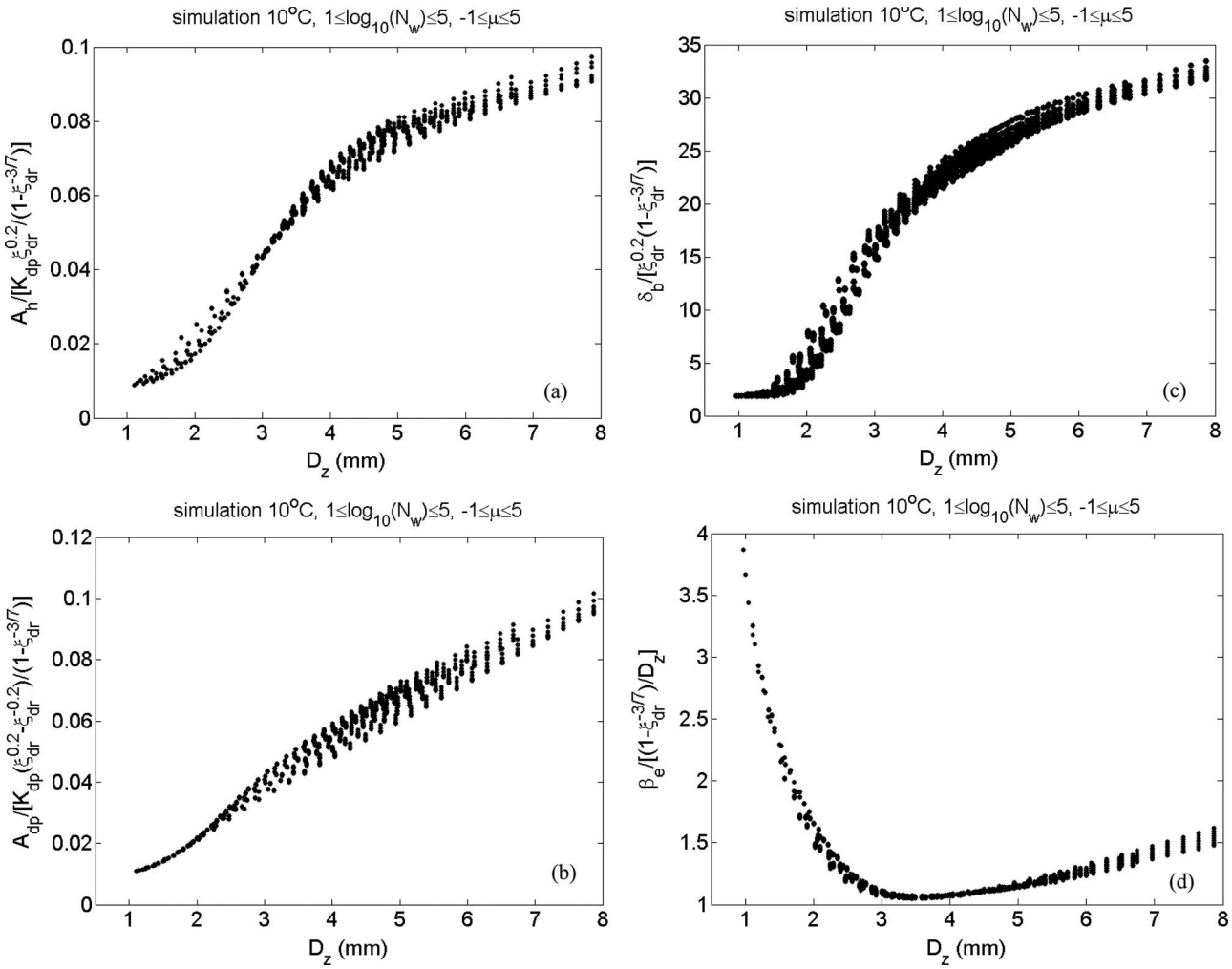

Fig. 2. Scaled (a) specific horizontal attenuation A_h(dB km^{-1}), (b) specific differential attenuation A_{dp}(dB km^{-1}), (c) backscattering differential phase shift δ_b (deg), and (d) effective mean slope parameter β_e(mm^{-1}) against reflectivity-weighted mean diameter D_z of raindrops from scattering simulations at X-band. The units of K_{dp} and Z_h are deg km^{-1} and mm^6 mm^{-3}, respectively, while ξ_{dr} (ratio) has no units.

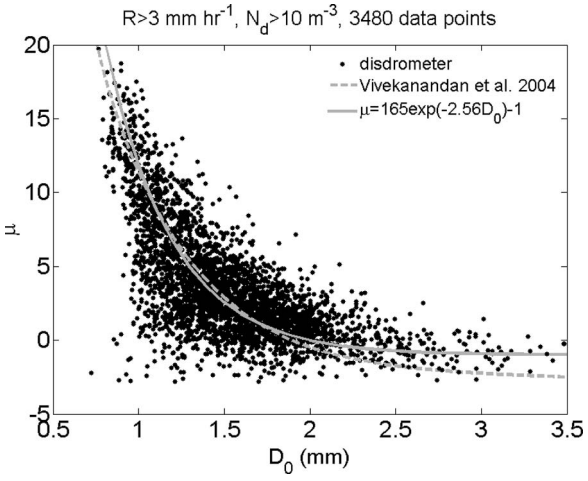

Fig. 3. Shape parameter of DSD μ against median volume diameter D_0 of raindrops from 1 min data of a video disdrometer operating in Athens, Greece area for 6 years in the time period 2002–2009.

Section III, least-squares estimators of D_z, D_0, N_w, β_e, R, A_h, A_{dp}, and δ_b were properly looked for. It was found that third-degree rational polynomial functions describe adequately the Mie character of scattering and include most of the dependence on D_z in the following form:

$$f_p(D_z) = \frac{\sum_{n=0}^{3} a_n D_z^n}{\sum_{n=0}^{3} b_n D_z^n} \tag{13}$$

where the subscript p indicates the corresponding rain parameter. The coefficients of the polynomials in the nominator and denominator of $f_p(D_z)$ are given in Table I for each relation rounded to four decimal digits for an accuracy in the calculation of the polynomials better than 1%. The coefficients a_0 and b_0 were forced to unity when such a fit was possible. The reflectivity-weighted mean diameter D_z (mm) has to be estimated first from the following nonlinear parameterized model:

$$D_z = D_{z1} f_{D_{z1}}(D_{z1})$$

$$D_{z1} = 0.1802 \left[\frac{Z_h}{K_{dp}} \xi_{dr}^{-0.2929} \left(1 - \xi_{dr}^{-0.4922}\right) \right]^{\frac{1}{3}} \tag{14a}$$

$$D_z = D_{z2} f_{D_{z2}}(D_{z2}),\ D_{z2} = 2.4780 \left(1 - \xi_{dr}^{-0.5089}\right). \tag{14b}$$

TABLE I
VALUES OF THE COEFFICIENTS OF THE RATIONAL POLYNOMIAL FUNCTIONS (13) IN THE PARAMETERIZATIONS OF RAIN PARAMETERS BY (14)–(21) AT X-BAND (9.37 g Hz) WITH 10 °C AIR TEMPERATURE AND CONSTRAINED μ BY (12)

Function	a_0/b_0	a_1/b_1	a_2/b_2	a_3/b_3
f_{Dz1} Eq. (14a)	0.9190/ 1.0000	0.1501/-0.2248	-0.1722/ 0.0182	0.0511/ 0.0238
f_{Dz2} Eq. (14b)	0.0546/ 0.0012	0.1056/ 0.0361	-0.1587/-0.0180	0.0976/-0.0084
f_{D0} in Eq. (15)	0.9542/ 1.0000	0.2989/ 0.2243	0.0577/ 0.2949	0.0030/-0.0053
f_{Nw1} in Eq. (16a)	1.0000/ 1.0000	-0.3487/-0.3689	-0.0185/-0.0256	0.0174/ 0.0234
f_{Nw2} in Eq. (16b)	1.0000/ 1.0000	-0.6792/-0.6410	0.2112/ 0.1551	-0.0109/-0.0065
f_{R1} in Eq. (17a)	-1.0000/ 1.0000	13.8906/ 11.825	-6.5271/-7.5152	1.2473/ 1.7780
f_{R2} in Eq. (17b)	1.0000/ 1.0000	-1.2313/-0.2176	2.1166/ 0.3064	0.6842/ 1.2305
$f_{\beta e1}$ in Eq. (18a)	-1.0000/-1.0000	3.0129/ 1.9617	-1.3370/-0.5870	0.2585/ 0.2953
$f_{\beta e2}$ in Eq. (18b)	1.0000/-1.0000	-0.3877/ 2.9798	-0.0801/-1.6281	0.0544/ 0.3232
$f_{\delta b}$ in Eq. (19)	-1.0000/ 1.0000	3.9903/-0.6011	-3.5131/ 0.0381	0.9494/ 0.0425
f_{Ah1} in Eq. (20a)	-1.0000/ 1.0000	4.2921/-1.0894	-3.8226/ 0.3431	1.0380/-0.0123
f_{Ah2} in Eq. (20b)	1.0000/ 1.0000	4.4689/-0.5402	-4.2310/ 0.1012	1.5102/ 0.0091
f_{Adp1} in Eq. (21a)	-1.0000/ 1.0000	5.2774/-0.5257	-2.3457/ 0.0948	0.3165/-0.0036
f_{Adp2} in Eq. (21b)	1.0000/ 1.0000	1.1659/-0.9058	-1.8684/ 0.2727	0.6931/-0.0044

Equation (14b) is valid only for the equilibrium value (0.066 mm^{-1}) of the slope parameter β_e and should be used only in case of missing or very low (and close to noise) K_{dp} measurements. The median volume diameter D_0 can be estimated from D_z either with an iterative method, using the equation $D_z = D_0(\mu+7)/(\mu+3.67)$ for the normalized Gamma DSD (as mentioned in Section III) and the constrained value of μ in (12), or using a polynomial approximation which is valid for the specific correlation of μ with D_0 (mm)

$$D_0 = D_z f_{D_0}(D_z). \tag{15}$$

For the parameters N_w(mm^{-1} m^{-3}), R(mm h^{-1}), and β_e(mm^{-1}), two parametric regressive models are derived

$$N_w = 1.0174 \left[\frac{Z_h}{F_6(\mu)}\right] \xi_{dr}^{-0.3822} D_0^{-7} f_{N_{w1}}(D_z) \tag{16a}$$

$$N_w = 3610 \left[\frac{K_{dp}}{\left(1-\xi_{dr}^{-0.3893}\right)}\right] D_0^{-4} f_{N_{w2}}(D_z) \tag{16b}$$

$$R = 0.8279 \left[\frac{F_R(\mu)}{F_6(\mu)}\right] Z_h \xi_{dr}^{-0.3779} D_0^{-2.33} f_{R1}(D_z) \tag{17a}$$

$$R = 0.8106 F_R(\mu) N_w D_0^{4.67} f_{R2}(D_0) \tag{17b}$$

$$\beta_e = 3.2241 \left[\frac{\left(1-\xi_{dr}^{-0.3636}\right)}{D_z}\right] f_{\beta_{e1}}(D_z) \tag{18a}$$

$$\beta_e = 444.16 \left(\frac{K_{dp}}{Z_h}\right) \xi_{dr}^{0.3819} D_z^2 f_{\beta_{e2}}(D_z) \tag{18b}$$

where $F_R(\mu) = 0.6 \times 10^{-3}\pi\, 3.78\, F_{3.67}(\mu)$ [1] and $f_{R2}(D_0)$ is a function of D_0. Equation (17b) is a straightforward derivation from the definition of rainfall rate with the addition of function $f_{R2}(D_0)$ to account for an exponential law which was used, instead of a power law for the terminal velocity of raindrops against their diameter [1]. Equations (16b) and (18b) basically include the direct use of K_{dp} (instead of including it only implicitly in D_z) in addition to Z_h and ξ_{dr}, but computationally are the same within the small error of parameterization (which is less than 5% as it is shown in the next section) as (16a) and (18b), respectively.

Similarly, the estimated approximations for δ_b (deg), A_h(dB km^{-1}), and A_{dp}(dB km^{-1}) are

$$\delta_b = 1.2891 \xi_{dr}^{0.3566} \left(1-\xi_{dr}^{-0.7447}\right) f_{\delta_b}(D_z) \tag{19}$$

$$A_h = 3.1482 \times 10^{-5} Z_h \xi_{dr}^{-0.1368} D_z^{-3} f_{A_{h1}}(D_z) \tag{20a}$$

$$A_h = 6.6888 \times 10^{-4} \left[\frac{K_{dp}\xi_{dr}^{0.3024}}{\left(1-\xi_{dr}^{-0.2107}\right)}\right] f_{A_{h2}}(D_z) \tag{20b}$$

$$A_{dp} = 3.1646 \times 10^{-5} Z_h \left(\xi_{dr}^{-0.1991} - \xi_{dr}^{-0.5254}\right) \times D_z^{-3} f_{A_{dp1}}(D_z) \tag{21a}$$

$$A_{dp} = 8.0295 \times 10^{-4} K_{dp} \left[\frac{\left(\xi_{dr}^{0.5025} - \xi_{dr}^{-0.5025}\right)}{\left(1-\xi_{dr}^{-0.2262}\right)}\right] \cdot f_{A_{dp2}}(D_z). \tag{21b}$$

As for (16b) and (18b), (20b) and (21b) basically include the direct use of K_{dp} in addition to Z_h and ξ_{dr}.

A. Effects of Variations of Air Temperature and Raindrop Axis Ratio

The parameterization functions given by (14)–(21) are tested using data from T-matrix scattering simulations at X-band like before with the addition of air temperature varying from 5 °C to 20 °C in increments of 5 °C (about 4900 data points for each value of air temperature) and the effect of raindrop oscillations on axis ratio according to [20] by adding a 15% random variability on axis ratio around r_e. This test aims to show the sensitivity of the derived parameterizations to these physical factors. The results are shown in Figs. 4 and 5. The additional subscript "e" in the y-axis labels indicates estimated parameters and the equality line (dashed) is also shown. For the rain parameters, where there are two proposed estimators, the one which includes directly K_{dp} and (17b) for R is only shown for brevity. In addition, estimations from other parameterizations at X-band found in the literature [13], [15], [26] are included where available.

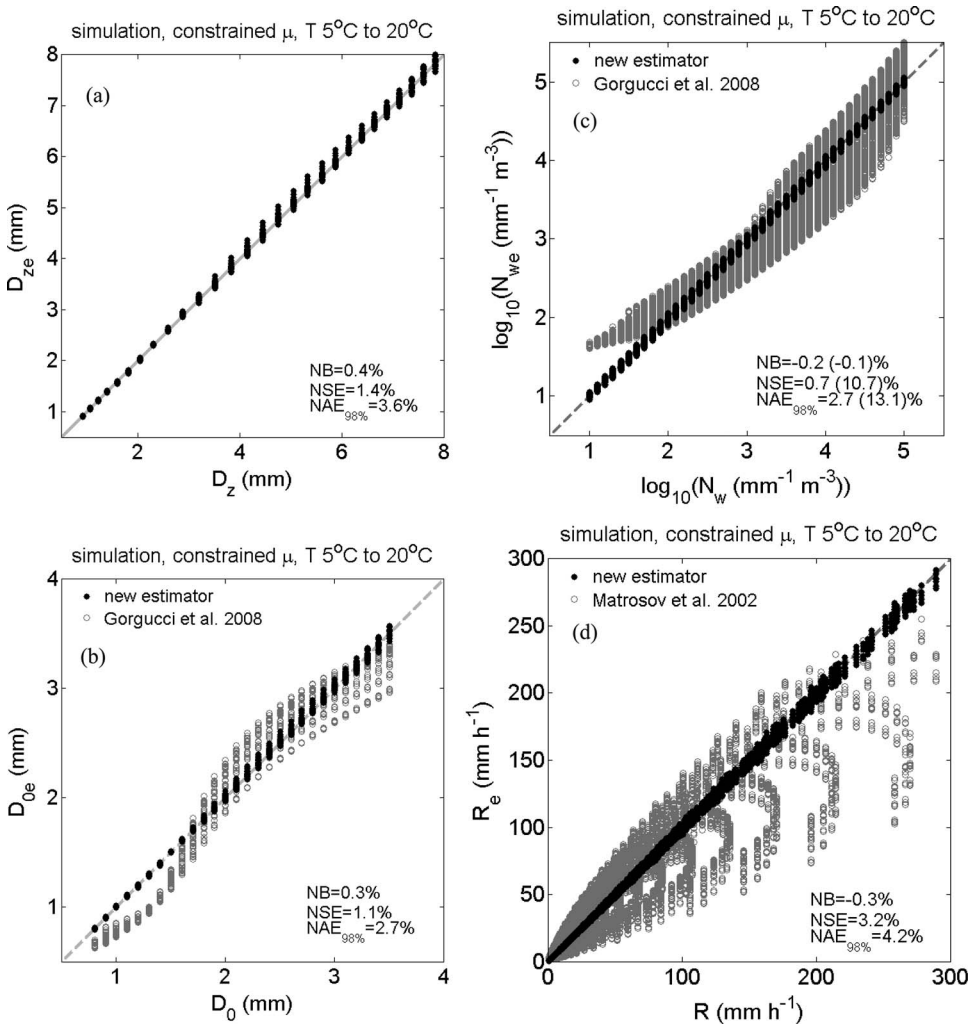

Fig. 4. Estimated (a) reflectivity-weighted mean diameter D_{ze} from (14a), (b) median volume diameter D_{0e} from (15), (c) DSD intercept parameter N_{we} from (16b), and (d) rainfall rate R_e from (17b) against reference values using scattering simulations at X-band. The parameterizations of Gorgucci *et al.* [13] and Matrosov *et al.* [15] are also shown for comparison.

Several error indexes were introduced to quantitatively analyze the results. The normalized mean bias (NB) and the normalized standard (root-mean-square) error (NSE) are used. NSE is the root-mean-square error normalized with respect to the mean reference value of the corresponding parameter and NB is the difference between the mean estimated and reference values normalized to the mean reference value. Reference values are the input values of the parameters in the simulations. The normalized absolute error $\mathrm{NAE}_{98\%}$ is the 98% percentile value of the absolute error normalized with the reference absolute value instead of the reference mean value, which should give too high NAE error at low absolute reference values. For this reason, only data points with absolute reference values greater than 10% of the mean of the absolute error were considered. $\mathrm{NAE}_{98\%}$ means that 98% of the data points are below this error value which, thus, is a measure of the maximum normalized absolute error excluding 2% of possible data outliers. In the case of N_w the NB, NSE, and $\mathrm{NAE}_{98\%}$ values are given for $\log_{10}(N_w)$ and also for N_w in parentheses.

Fig. 4(a) and (b) shows the parameterizations of Dz and D0 obtained using (14a) and (15), respectively, against the corresponding reference values. Both parameterizations show linear behavior and little scatter against the reference values. The parameterization of D_0 from [13] shows nonlinear behavior and significant scatter as it was also observed in that paper for a smaller range of air temperatures, rain parameters D_0, N_w, and β_e and for μ in the range -1 to 5 instead of a constrained μ (range of values -1 to 20). If only the data with the ranges of reference rain parameters and physical constraints as in [13] are kept in the comparison, then their parameterization shows good agreement with the reference values as presented in that paper. The better performance of (15) for a wider range of rain parameters is expected as it is optimized for the form of the dependence on radar measurements and the Mie character of scattering. Similar remarks can be done for N_w estimated from (16b) and shown in Fig. 4(c). The new parameterization gives very small error even for the value of N_w itself (statistics shown in parentheses) and a direct comparison of N_w instead of $\log 10(N_w)$ shows good results, while in literature only the comparison of $\log 10(N_w)$ with the reference value is met. The parameterization of rainfall rate by (17b) shown in Fig. 4(d) also presents very small error, while the one from [15]

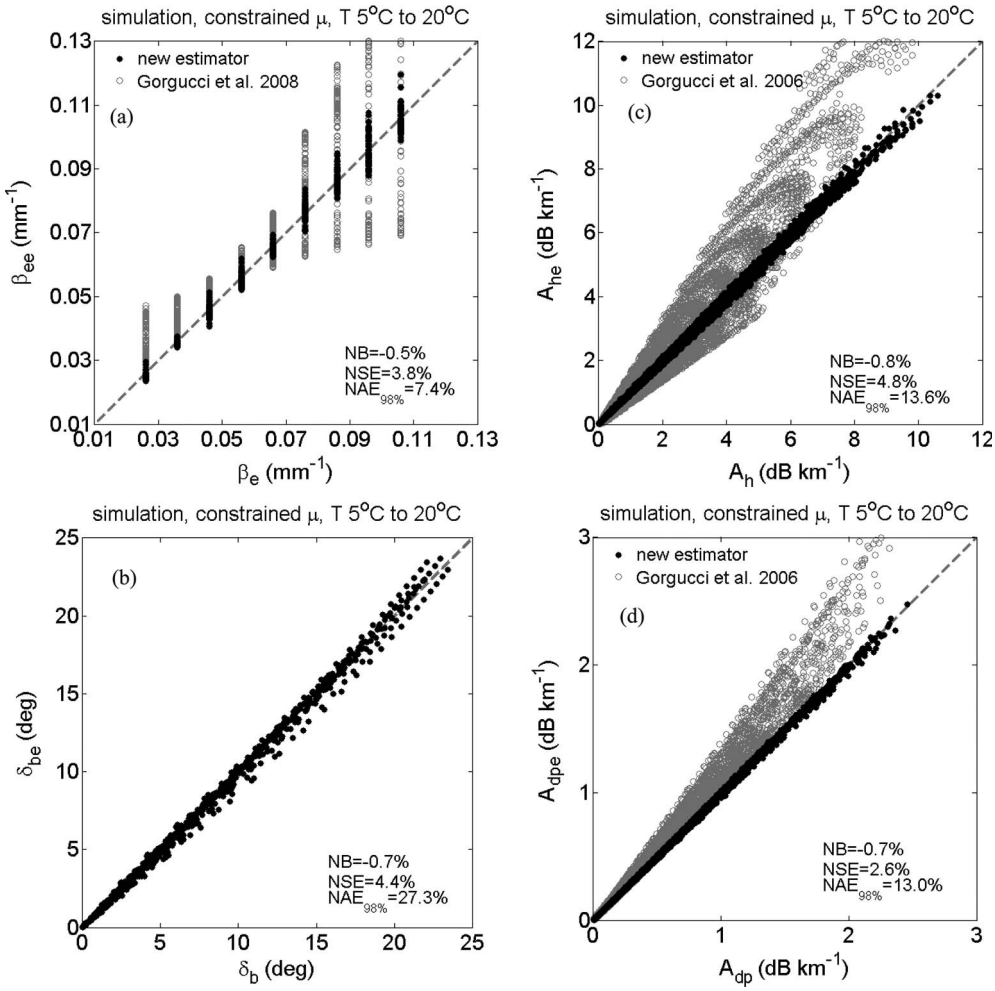

Fig. 5. Estimated (a) effective mean slope parameter β_{ee} from (18b), (b) backscattering differential phase shift δ_{be} from (19), (c) specific horizontal attenuation A_{he} from (20b), and (d) specific differential attenuation A_{dpe} from (21b) against reference values using scattering simulations at X-band. The parameterizations of Gorgucci *et al.* [26] are also shown for comparison.

shows considerable scatter for the same reasons (non-optimal parameterization, wider range of reference rain parameters in simulations) as mentioned above.

Fig. 5 shows the results for the rest of the rain parameters (i.e., β_e, δ_b, A_h, and A_{dp}), where the estimated values come from (18b), (19), (20b), and (21b), respectively. The last three parameters are useful for the development of attenuation correction algorithms of radar measurements in rain, which is the subject of another paper [27]. It should be noted that the approximation error of the new algorithm is very low, compared to other estimators in the literature that show significant scatter. Thus, in total Figs. 4 and 5 show that with respect to simulated data for the constrained μ according to disdrometer observations and under a wide range of physical parameters (including air temperature and physical variations of raindrop axis ratio) the proposed parameterizations are characterized by very small errors. It should be noted that as it was shown in Section III, the estimation of the parameters D_0, N_w, μ, and rainfall rate R in the parameterizations presented in this work depends on the observed constraining function of μ against D_0. However, as discussed in Section III (Figs. 1 and 2) the functional forms of D_z, β_e, A_h, A_{dp}, and δ_b against radar observables are independent (within the small error of the parameterizations) of the shape parameter μ and are represented by (14) and (18)–(21). Thus, the $\mu - D_0$ constraint does not affect the estimation of these parameters, which makes their estimation and attenuation correction schemes that are based on these parameterizations more robust and less susceptible to the physical variability of μ.

B. Effects of Radar Calibration Bias and Measurement Noise

In real radar measurements, there are error factors which could affect the performance of the parameterizations like the calibration biases and random measurement errors. Their effect is examined below in a simulation experiment by adding systematic and random errors to the simulated Z_h, Z_{dr}, and K_{dp} data. Synthetic data are used instead of real radar data to evaluate the performance of the parameterizations in a wider range of rain parameters compared to available radar data and to avoid additional significant effects such as rain-path attenuation and issues due to radar volume versus point measurement scale mismatch and spatial separation. This kind

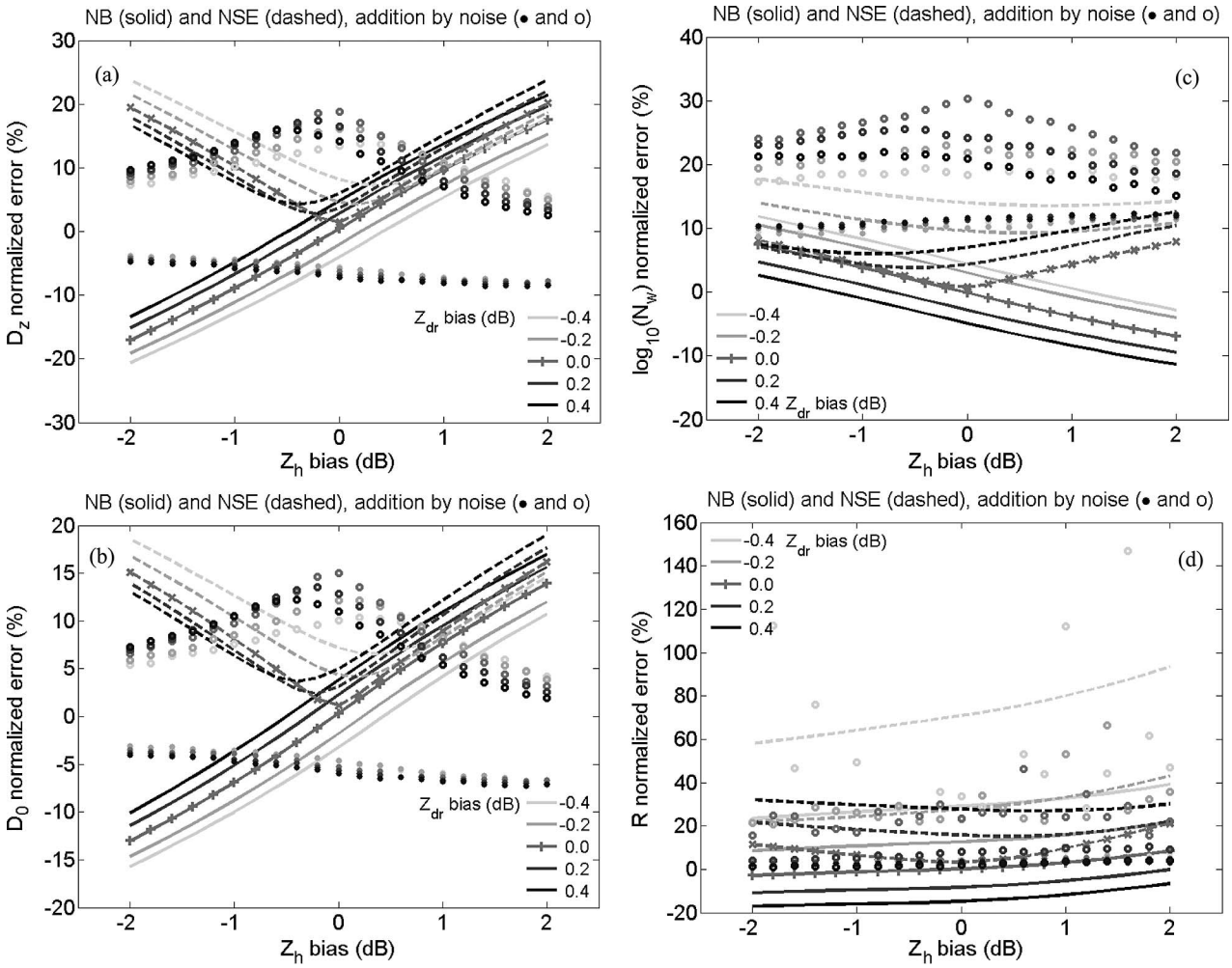

Fig. 6. As in Fig. 4 but for NB and NSE errors in the presence of bias in Z_h (solid lines) and Z_{dr} (dashed lines) and the additional errors (filled circles for NB and open circles for NSE) when random noise is also added to Z_h, Z_{dr}, and K_{dp} with standard deviation 1 dB, 0.2 dB, and 0.3 deg km^{-1}, respectively. Crosses in lines indicate zero bias of Z_{dr}.

of overall evaluation of the performance of the parameterizations presented in this work in comparison with other parameterizations found in literature is examined in detail in [28]. The typical standard error (measurement noise) in radar measurements of Z_h, Z_{dr}, and K_{dp} is 1 dB, 0.2 dB, and 0.3 deg km^{-1}, respectively. This noise was simulated by adding a Gaussian random noise with these standard deviations to the corresponding simulated variables and then (14)–(21) were used for the estimation of rain parameters. Due to the addition of noise, the practical constraint [see (11)] of the lower limit of K_{dp} for useable simulation data was set to 0.3 deg km^{-1}. Calibration bias errors were simulated by adding an offset to Z_h and Z_{dr}.

Figs. 6 and 7 show the sensitivity of the parameterizations to both bias and noise errors in input variables. Lines (solid for NB, dashed for NSE) represent the errors in the presence only of bias errors against Z_h bias (-2 to 2 dB) and for different values of Z_{dr} bias (-0.4 to 0.4 dB). Filled and open circles represent the increase of NB and NSE, respectively, when measurement noise is added in addition to calibration biases. In general, NB errors show the most significant dependence on calibration biases as expected with values from -20 to 20%, at extreme calibration bias errors considered in this study, while NB is the least sensitive to measurement noise with absolute values below 10%. NSE by calibration biases shows a minimum below 5% at zero calibration biases (as shown in Figs. 4 and 5) and maximum values up to 20–30% at extreme calibration biases. NSE by measurement noise shows some variation with calibration biases with maximum values of 10 to 30% usually at zero calibration biases. The parameterization of rainfall rate is the only one which shows very high NB and NSE (more than 50%) at Z_{dr} bias of -0.4 dB. At this value of Z_{dr} bias the NSE in the estimation of A_h is also high above 50%. These high sensitivities have to do with the form of dependence of the corresponding parameterization function on ξ_{dr}. For typical values of 1 and 0.2 dB for Z_h and Z_{dr} calibration biases the NB and NSE errors in parameterizations are generally less than 20%, which shows that they have an acceptable sensitivity to calibration biases and measurement noise. It should be noted that these NB and NSE errors are for the simulations carried out over a wider range of reference rain parameters compared to literature as mentioned in Section IV-A, which leads to an increment of NB and NSE errors compared to less narrow ranges of rain parameters.

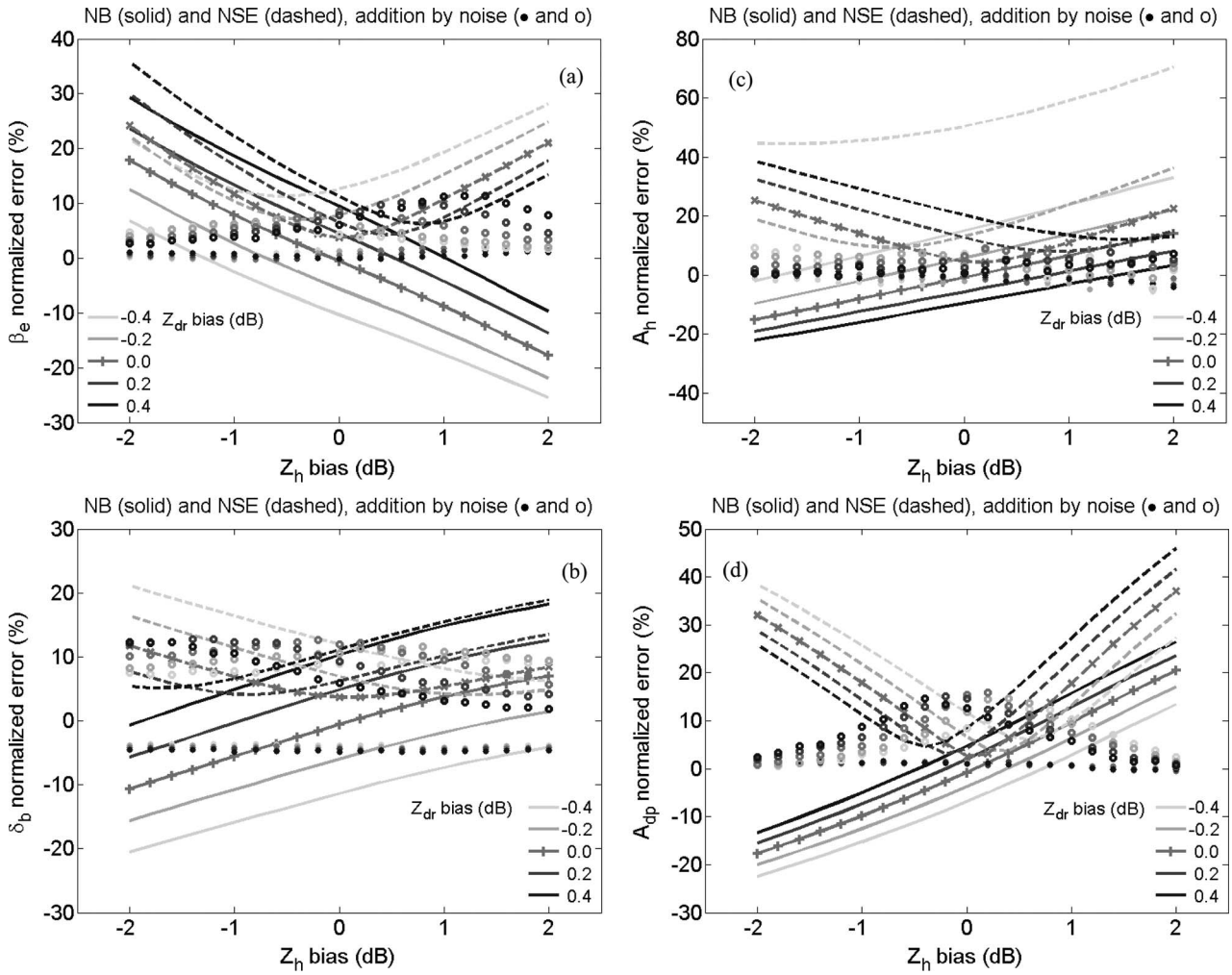

Fig. 7. As in Fig. 6 but for the parameterizations shown in Fig. 5.

C. Evaluation With Disdrometer Data (DSD Physical Variability)

In this section, the parameterizations are evaluated against the disdrometer data set mentioned in Section III. The disdrometer data include the physical variations of DSD (i.e., observed DSDs have random variability around a normalized Gamma distribution) and, thus, the μ parameter is not constrained but varies according to measurements. However, it should be noted that μ is not a random variable but shows random variations (Fig. 3) around the constraining function (12). Figs. 8–10 are scatter plots of estimated against disdrometer values or rain parameters. The disdrometer observations which were more reliable and less affected by measurement noise where D_0, N_w, and μ, even though the 2-D-VD disdrometer can provide estimates of raindrop axis ratio, canting angle, and fall velocity. The latter parameters were defined as in the simulations in Section IV-A. The disdrometer values of δ_b, A_h, and A_{dp} were calculated from the disdrometer DSDs and T-matrix scattering routines. The input variables in the parameterizations Z_h, Z_{dr}, and K_{dp} were also calculated from T-matrix scattering calculations for the same range of air temperature values (5 °C to 20 °C) as in Section IV-A.

According to Figs. 8 and 9, the performance of the parameterizations is quite good with correlation coefficients above 0.9, very low NB (less than 5%), increased NSE errors (10 to 20%) compared to simulations in Figs. 4 and 5 and relatively high $\mathrm{NAE}_{98\%}$ errors up to 50%. The parameterization of μ in Fig. 10 shows the higher NSE and $\mathrm{NAE}_{98\%}$ (33 and 68%, respectively). These higher random errors are expected due to the physical variability in disdrometer DSDs, but also due to measurement errors. The estimates from corresponding parameterizations found in literature (where available) are also shown. In the case of β_e parameterization, the mean and standard error of the parameterization by [13] are also shown at points shifted to the right on the x-axis by 0.002 mm^{-1} to better distinguish the trend and the error of this parameterization which shows a higher scatter. Similar to the simulations results in Figs. 4 and 5, these parameterizations from the available literature show considerable higher biases and scatter compared to the new parameterizations. However, it should be noted again that these parameterizations were developed and tested in narrower ranges of values of rain parameters compared to the ranges of values used in the present work.

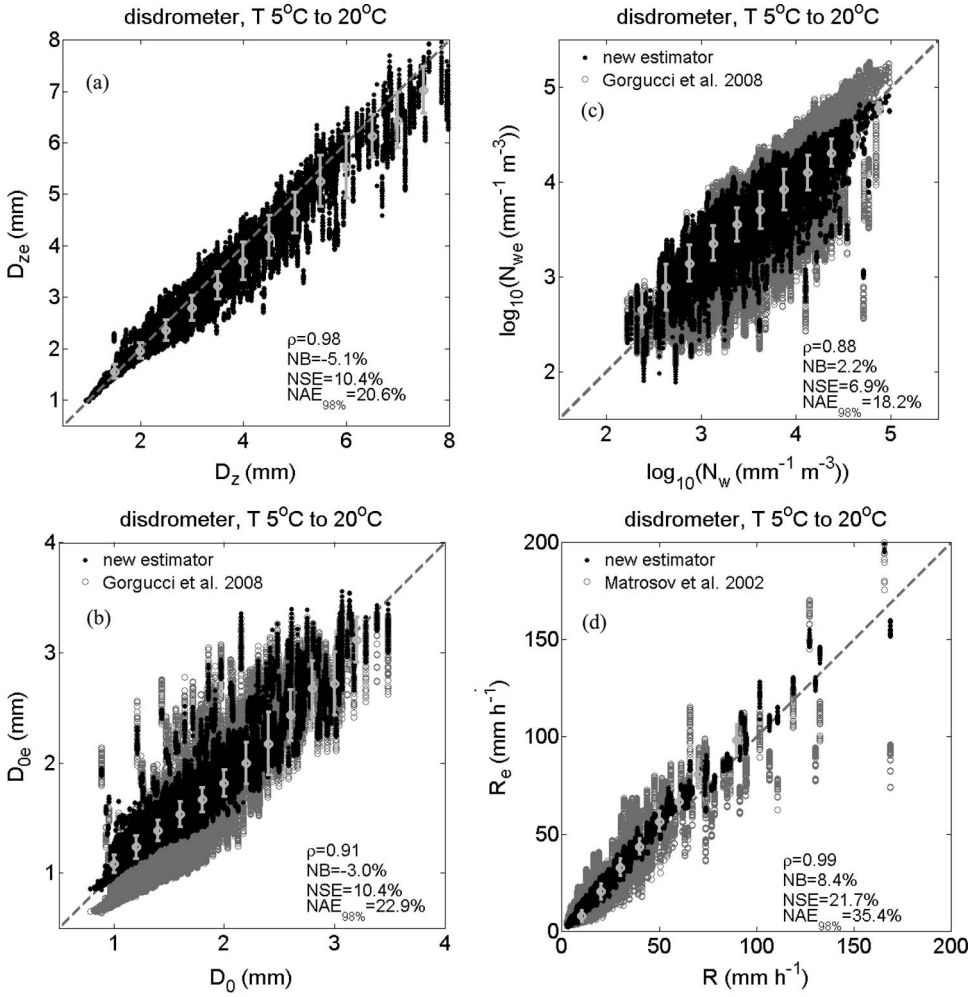

Fig. 8. As in Fig. 4 but for disdrometer DSD data instead of simulated normalized gamma DSD with constrained μ. The mean (open circles) and standard error of estimations in bins and the correlation coefficient ρ are also shown.

V. Summary and Conclusions

A new methodology to define minimum error parameterizations of rain microphysical parameters, rainfall rate, radar specific path attenuation, and backscattering phase shift in rain from polarimetric radar products was presented. To describe the effect of the Mie character of rain scattering, the proposed method is based on the functional relations valid at the theoretical Rayleigh scattering limit with the addition of a multiplicative factor (rational polynomial) as a function of reflectivity-weighted diameter. The coefficients in the parameterizations were estimated by minimum-mean-square fit of T-matrix scattering simulation data over a wide range of rain parameters. The use of raindrop reflectivity-weighted diameter in the multiplicative factors was found to minimize the effect of the shape parameter of the DSD on most of the model parameterizations. Based on disdrometer measurements, the shape parameter of the DSD was constrained to an exponential relationship of raindrop median volume diameter. In this way the retrieval ambiguity due to the fact that there are more independent rain parameters to estimate (N_w, D_0, μ, and β_e) than the three (Z_h, Z_{dr}, and K_{dp}) considered radar measurements was basically removed.

The functional dependence of the DSD shape parameter μ on median volume diameter D_0 may lead to changes in the constants of the proposed parameterizations if it is quite different than the one found by the disdrometer data used in this study. However, a similar dependence of μ on D_0 has been found from other researchers in different climatic regimes and it seems to be an inherent property of rain DSDs. It should be noted that as it was shown in this work the estimation of D_z, β_e, A_h, A_{dp}, and δ_b, which can be used in attenuation correction schemes, from radar observables is independent of the constraining function of μ against D_0. Other available information might be used to remove the $\mu - D_0$ constraint, but the co-polar correlation coefficient ρ_{hv}, which is usually available from polarimetric radars does not have significant dependence on μ separately from its direct dependence on D_z and Z_{dr} to remove this constraint in practice.

The proposed regressive parameterizations, developed for X-band polarimetric radars, were tested with a simulation sensitivity analysis for the effects of air temperature, raindrop oscillations, radar calibration biases and measurement noise and compared to existing parameterizations in the literature. In addition, they were tested against long-term observational

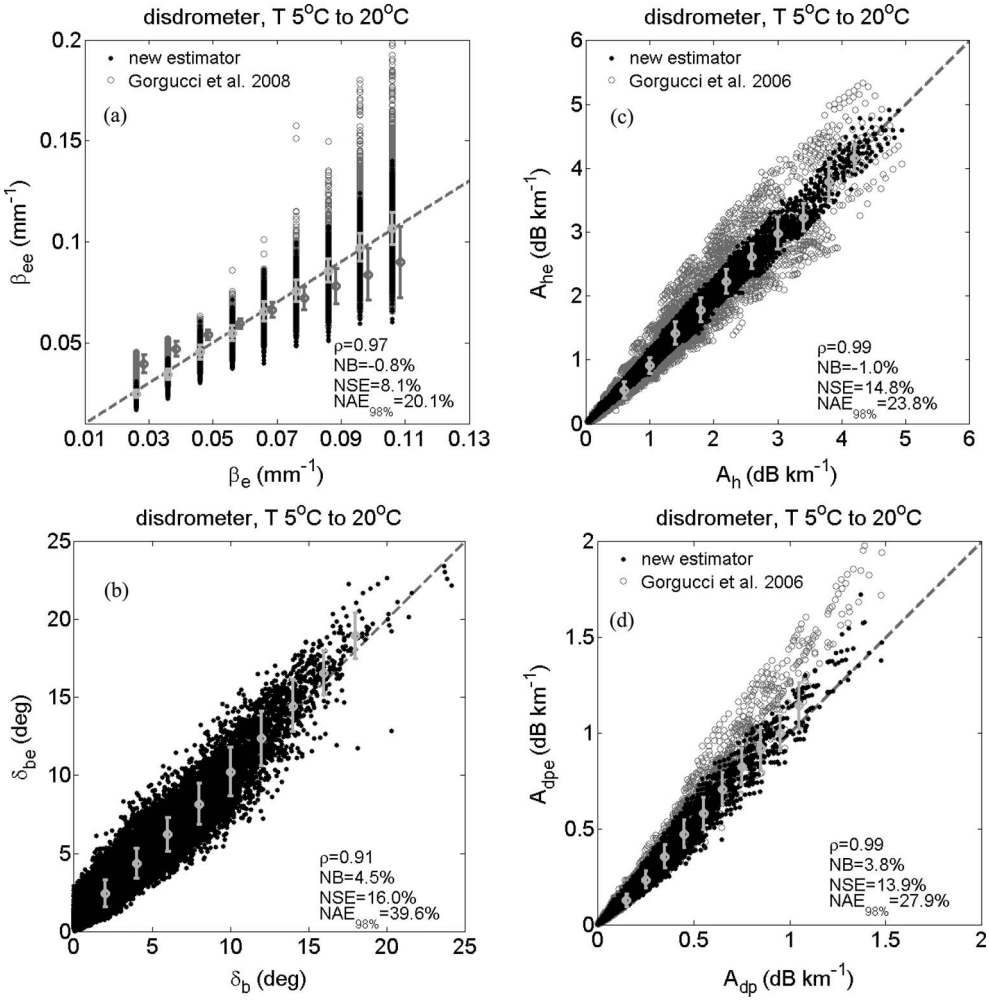

Fig. 9. As in Fig. 5 but for disdrometer DSD data instead of simulated normalized gamma DSD with constrained μ. The mean (open circles) and standard error of estimations in bins and the correlation coefficient ρ are also shown.

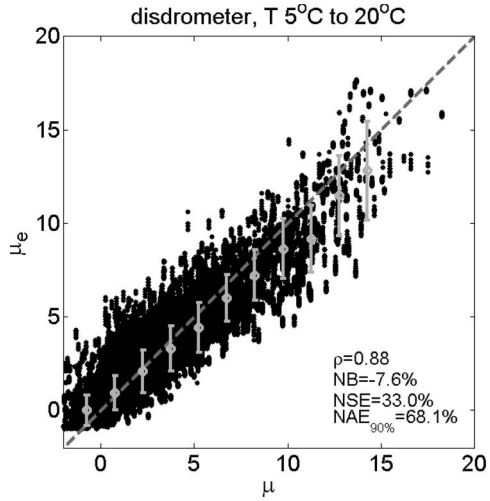

Fig. 10. Estimated shape parameter μ_e from (12) with D_0 estimated from (15) against the reference value from disdrometer DSD data.

data from a 2-D-VD disdrometer. The new parameterizations show low sensitivity to the variations of physical parameters, very low bias approximation errors and medium sensitivity (typically less than 20% errors) to usual radar calibration and measurement noise. The error of the parameterizations could be reduced to about 5% as the measurement errors due radar calibration and measurement reduce with advances in radar technology. The parameterizations of radar specific path attenuation and backscattering phase shift could be applied in schemes of correction of attenuation of the radar signal in rain, which is quite significant at X-band. The coefficients of the parameterizations presented in this paper are valid for X-band and within the wide range of variability of the various rain microphysics and atmospheric conditions considered here, but the methodology presented here can be applied to C-band as well as higher frequencies. It is also the intention of the authors to apply of the proposed Mie-parameterized retrieval methodology to the global precipitation measurement mission satellite-based dual-frequency Ku- and Ka-band radar [29]. Future extensions of this study should include independent verification of these findings based on high-quality ground validation data from different hydro-climatic regimes.

REFERENCES

[1] V. N. Bringi and V. Chandrasekar, *Polarimetric Doppler Weather Radar: Principles and Applications*. Cambridge, U.K.: Cambridge Univ. Press, 2001, p. 636.

[2] T. A. Seliga and V. N. Bringi, "Potential use of the reflectivity at orthogonal polarizations for measuring precipitation," *J. Appl. Meteorol.*, vol. 15, no. 1, pp. 69–76, 1976.

[3] V. N. Bringi, V. Chandrasekar, and R. Xiao, "Raindrop axis ratio and size distributions in Florida rainshafts: An assessment of multiparameter radar algorithms," *IEEE Trans. Geosci. Remote Sens.*, vol. 36, no. 3, pp. 703–715, May 1998.

[4] V. N. Bringi, V. Chandrasekar, J. Hubbert, E. Gorgucci, W. L. Randeu, and M. Schoenhuber, "Raindrop size distribution in different climatic regimes from disdrometer and dual-polarized radar analysis," *J. Atmos. Sci.*, vol. 60, no. 2, pp. 354–365, Jan. 2003.

[5] P. T. Willis, "Functional fits to some observed drop size distribution and parameterization of rain," *J. Atmos. Sci.*, vol. 41, no. 9, pp. 1648–1661, 1984.

[6] A. J. Illingworth and T. M. Blackman, "The need to represent raindrop size spectra as normalized gamma distributions for the interpretation of polarization radar observations," *J. Appl. Meteorol.*, vol. 41, no. 3, pp. 286–297, Mar. 2002.

[7] V. N. Bringi, T. Keenan, and V. Chandrasekar, "Correcting C-band radar reflectivity and differential reflectivity data for rain attenuation: A self consistent method with constraints," *IEEE Trans. Geosci. Remote Sens.*, vol. 39, no. 9, pp. 1906–1915, Sep. 2001.

[8] E. Gorgucci, V. Chandrasekar, V. N. Bringi, and G. Scarchilli, "Estimation of raindrop size distribution parameters from polarimetric radar measurements," *J. Atmos. Sci.*, vol. 59, no. 15, pp. 2373–2384, Aug. 2002.

[9] E. A. Brandes, G. Zhang, and J. Vivekanandan, "An evaluation of a drop distribution-based polarimetric radar rainfall estimator," *J. Appl. Meteorol.*, vol. 42, no. 5, pp. 652–660, 2003.

[10] S. Park, V. N. Bringi, V. Chandrasekar, M. Maki, and K. Iwanami, "Correction of radar reflectivity and differential reflectivity for rain attenuation at X-band, Part I: Theoretical and empirical basis," *J. Atmos. Ocean. Technol.*, vol. 22, no. 11, pp. 1621–1632, Nov. 2005.

[11] S. Park, M. Maki, K. Iwanami, V. N. Bringi, and V. Chandrasekar, "Correction of radar reflectivity and differential reflectivity for rain attenuation at X-band, Part II: Evaluation and application," *J. Atmos. Ocean. Technol.*, vol. 22, no. 11, pp. 1633–1655, Nov. 2005.

[12] E. Gorgucci and L. Baldini, "Attenuation and differential attenuation correction of C-band radar observations using a fully self-consistent methodology," *IEEE Geosci. Remote Sens. Lett.*, vol. 4, no. 2, pp. 326–330, Apr. 2007.

[13] E. Gorgucci, V. Chandrasekar, V. N. Bringi, and L. Baldini, "Microphysical retrievals from dual-polarization radar measurements at X band," *J. Atmos. Ocean. Technol.*, vol. 25, no. 5, pp. 729–741, May 2008.

[14] F. S. Marzano, G. Botta, and M. Montopoli, "Iterative Bayesian retrieval of hydrometeor content from X-band polarimetric weather radar," *IEEE Trans. Geosci. Remote Sens.*, vol. 48, no. 8, pp. 3059–3074, Aug. 2010.

[15] S. Matrosov, K. Clark, B. Martner, and A. Tokay, "X-band polarimetric radar measurements of rainfall," *J. Appl. Meteorol.*, vol. 41, no. 9, pp. 941–952, Sep. 2002.

[16] E. N. Anagnostou, M. N. Anagnostou, W. Krajewski, A. Kruger, and B. Miriovsky, "High-resolution rainfall estimation from X-band polarimetric radar measurements," *J. Hydrometeorol.*, vol. 5, no. 1, pp. 110–128, 2004.

[17] C. W. Ulbrich, "Natural variations in the analytical form of the drop size distribution," *J. Clim. Appl. Meteorol.*, vol. 22, pp. 1764–1775, 1983.

[18] J. Testud, E. Le Bouar, E. Obligis, and M. Ali-Mehenni, "The rain profiling algorithm applied to polarimetric weather radar," *J. Atmos. Ocean. Technol.*, vol. 17, no. 3, pp. 332–356, Mar. 2000.

[19] K. V. Beard and C. Chuang, "A new model for the equilibrium shape of raindrops," *J. Atmos. Sci.*, vol. 44, no. 11, pp. 1509–1524, 1987.

[20] M. Thurai, M. Szakall, V. N. Bringi, K. V. Beard, S. K. Mitra, and S. Borrmann, "Drop shapes and axis ratio distributions: Comparison between 2-D video disdrometer and wind-tunnel measurements," *J. Atmos. Ocean. Technol.*, vol. 26, no. 7, pp. 1427–1432, 2009.

[21] K. V. Beard and A. R. Jameson, "Raindrop canting," *J. Atmos. Sci.*, vol. 40, no. 2, pp. 448–454, 1983.

[22] P. C. Waterman, "Symmetry, unitarity, and geometry in electromagnetic scattering," *Phys. Rev. D*, vol. 3, no. 4, pp. 825–839, 1971.

[23] M. I. Mishchenko, "Calculation of the amplitude matrix for a nonspherical particle in a fixed orientation," *Appl. Opt.*, vol. 39, no. 6, pp. 1026–1031, Feb. 2000.

[24] G. Zhang, J. Vivekanandan, and E. Brandes, "A method for estimating rain rate and drop size distribution from polarimetric radar measurements," *IEEE Trans. Geosci. Remote Sens.*, vol. 39, no. 4, pp. 830–841, Apr. 2001.

[25] J. Vivekanandan, G. Zhang, and E. Brandes, "Polarimetric radar estimators based on a constrained gamma drop size distribution model," *J. Appl. Meteorol.*, vol. 43, no. 2, pp. 217–230, Feb. 2004.

[26] E. Gorgucci, V. Chandrasekar, and L. Baldini, "Correction of X-band radar observation for propagation effects based on the self-consistency principle," *J. Atmos. Ocean. Technol.*, vol. 23, no. 12, pp. 1668–1681, Dec. 2006.

[27] J. Kalogiros, M. N. Anagnostou, E. N. Anagnostou, M. Montopoli, E. Picciotti, and F. S. Marzano, "Evaluation of a new polarimetric algorithm for rain path attenuation correction of X-band radar observations against disdrometer data," *IEEE Trans. Geosci. Remote Sens.*, 2012.

[28] M. N. Anagnostou, J. Kalogiros, F. S. Marzano, E. N. Anagnostou, M. Montopoli, and E. Picciotti, "Performance evaluation of a new rain microphysics algorithm for dual-polarization X-band radars using long-term radar and disdrometer measurements," *J. Hydrometeorol.*, 2012.

[29] A. Y. Hou, G. S. Jackson, C. D. Kummerow, and J. M. Shepherd, "Global precipitation measurement," in *Precipitation: Advances in Measurement, Estimation, and Prediction*, S. Michaelides, Ed. Berlin, Germany: Springer-Verlag, 2008, pp. 131–164.

John Kalogiros received the B.Sc., M.Sc., and Ph.D. degrees from the University of Athens, Athens, Greece, in 1989, 1991, and 1997, respectively.

During the time period 2000–2002, he was a Research Assistant in the Naval Postgraduate School, Monterey, CA. Currently, he is an Assistant Researcher in the Institute of Environmental Research and Sustainable Development, National Observatory of Athens, Athens, Greece. His research interests and accomplishments lie in the areas of polarimetric weather radar, acoustic sounder (sodar), aircraft and ground-based measurements of the atmospheric boundary layer.

Marios N. Anagnostou received the M.Eng. degree in avionics from York University, York, U.K. and the Ph.D. degree from the University of Connecticut, Storrs.

His major research involvement is to implement and validate new advanced dual-polarization X-band algorithms on rainfall microphysics focused on mountainous and urban basins for high-resolution precipitation observation and estimation and flash-flood prediction. He has been awarded a Group Achievement Award by NASA for the best group performance and the high quality of data collected in CAMEX field experiment, in 2002, and a European Union Marie Curie Intra-European Fellowship, in 2009.

Emmanouil N. Anagnostou received the B.S. degree from the National Technical University, Athens-Greece, in 1990, and the M.S. and Ph.D. degrees from the University of Iowa, Iowa City, in 1994 and 1997, respectively, all in civil and environmental engineering.

Currently, he is an Endowed Chair Professor in the Department of Civil and Environmental Engineering and the Director of the Environmental Engineering Program at the University of Connecticut, Storrs. His research interests are the development of techniques for remote sensing of precipitation parameters from satellite and ground-based sensors and the integration of rainfall remote sensing products in hydrologic modeling for the prediction of floods and the study of regional water cycle.

Mario Montopoli received the Laurea degree in electronic engineering from the University of L'Aquila, L'Aquila, Italy, in 2004, and the Ph.D. degree in radar meteorology from the University of Basilicata, Potenza, Italy, and the University of Rome "La Sapienza," Rome, Italy, in 2008, through a joint program.

Since 2005, he has been with the Centro di Eccellenza per l'integrazione di tecniche di Telerilevamento E Modellistica numerica per la Previsione di eventi meteorologici Severi, University of L'Aquila, where he is currently a Research Scientist on ground-based radar meteorology, with a special focus on C-band applications and processing techniques. Since 2006, he has also been a Research Assistant with the Department of Electrical and Information Engineering, University of L'Aquila.

Errico Picciotti received the the Laurea degree *(cum laude)* in electrical engineering from the University of Ancona, Ancona, Italy, in 1993.

In 1997, he was with the Science and Technology Park of Abruzzo, L Aquila, Italy, as a Radar Meteorologist. In 2002, he was a Researcher with the Centro di Eccellenza per l integrazione di Tecniche di Telerilevamento e Modellistica Numerica per la Previsione di Eventi Meteorologici Severi, University of L Aquila, L Aquila, Italy, where he worked on radar systems and polarimetry. Since 2007, he has been with HIMET, L Aquila, where he is the Coordinator of the Radar Meteorology Division.

Frank Silvio Marzano (S'89–M'99–SM'03) received the Laurea degree *(cum laude)* in electronic engineering, in 1988, and the Ph.D. degree, in 1993, in applied electromagnetics both from the Sapienza University of Rome, Italy.

After being with the Italian Space Agency and a Lecturer at the University of Perugia, Italy, in 1997, he joined the Department of Electrical Engineering and in 2001 cofounded the Center of Excellence [Centro di Eccellenza per l'integrazione di tecniche di Telerilevamento E Modellistica numerica per la Previsione di eventi meteorologici Severi (CETEMPS)], University of L Aquila, Italy. In 2005, he joined the Department of Electronic Engineering (now Department of Information Engineering), Sapienza University of Rome, Italy where he presently teaches courses on antenna theory, electromagnetic propagation, and remote sensing. Since 2007, he has also been the Vice-director of CETEMPS, University of L Aquila, Italy. His current research concerns passive and active remote sensing of the atmosphere, development of inversion methods, radiative transfer modeling, and radar meteorology. He is also involved in radio and optical propagation topics in relation to incoherent wave modeling, scintillation prediction, and rain fading analysis. Since January 2004, he has been acting as an Associate Editor of IEEE GEOSCIENCE REMOTE SENSING LETTERS. Since 2011, he has also been an Associate Editor of EGU *Atmospheric Measurement Techniques* journal.

Dr. Marzano is a Fellow of the Royal Meteorological Society, a Senior Member of the IEEE Geoscience and Remote Sensing Society, and a member of the American Meteorological Society. In 1993, he received the Young Scientist Award of XXIV General Assembly of URSI (Osaka, Japan). In 2008 and 2011, he received the Best Paper Award from the EGU-Plinius Conferences in Nicosia (Cyprus) and Savona (Italy), respectively, and in 2009 the Best Oral Paper Award on propagation from the EuCAP Conference (Berlin, Germany). Within 2001–2012, he was the Italian national delegate for the European COST actions n. 720, n. 280 and n. ES702, and n. IC0802 PropTNEO. Since 2011, he has been the national vice-delegate for the COST Action project IC1101 OpticWISE. He is also a member of the Science team of the Global Precipitation Mission, a member of the European Volcanic Ash Cloud Expert Group, and a member of EuMetSat Precipitation Science Advisory Group.